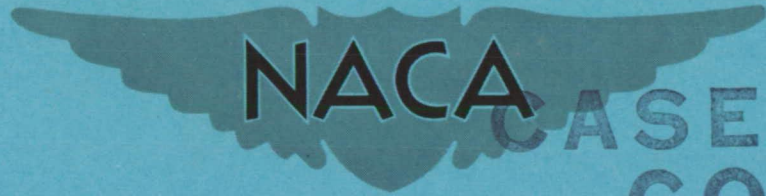


CONFIDENTIAL

Copy 426
RM L56F07a



NACA CASE FILE COPY
RESEARCH MEMORANDUM

RESULTS FROM AN INVESTIGATION IN ROUGH AIR AT MACH
NUMBERS FROM 0.84 TO 1.67 OF A TAILLESS ROCKET
MODEL HAVING 60° TRIANGULAR WINGS

By A. James Vitale

Langley Aeronautical Laboratory
Langley Field, Va.

CLASSIFIED DOCUMENT

This material contains information affecting the National Defense of the United States within the meaning
of the espionage laws, Title 18, U.S.C., Secs. 793 and 794, the transmission or revelation of which in any
manner to an unauthorized person is prohibited by law.

CLASSIFICATION CHANGED TO UNCLASSIFIED
AUTHORITY: NACA RESEARCH ABSTRACT NO. 228
EFFECTIVE DATE: JUNE 24, 1958
WHL

**NATIONAL ADVISORY COMMITTEE
FOR AERONAUTICS**

WASHINGTON

July 26, 1956

CONFIDENTIAL

NATIONAL ADVISORY COMMITTEE FOR AERONAUTICS

RESEARCH MEMORANDUM

RESULTS FROM AN INVESTIGATION IN ROUGH AIR AT MACH

NUMBERS FROM 0.84 TO 1.67 OF A TAILLESS ROCKET

MODEL HAVING 60° TRIANGULAR WINGS

By A. James Vitale

SUMMARY

Results from a flight investigation in continuous rough air at Mach numbers from 0.84 to 1.67 are presented for a tailless rocket model having cruciform 60° triangular wings. The variation of root-mean-square acceleration increment with Mach number indicated a rapid increase of roughly 100 percent as the Mach number increased from 0.90 to 1.00. Of this 100 percent, about 70 percent appeared to be associated with the rapid decrease in pitch damping over this Mach number range. From Mach numbers 1.02 to 1.67, the experimental data showed little variation with Mach number at least within the estimated accuracy of the results of ± 20 percent.

INTRODUCTION

The need for experimental data at transonic and supersonic speeds on the response of airplanes and missiles to gusts and associated gust loads led to the development of a program which utilizes rocket-powered models for rough-air tests. Previous rocket model tests in rough air have covered the Mach number range of about 0.66 to 1.02, as described in references 1, 2, and 3. These tests provided useful data on the effects of changes in configuration and dynamic longitudinal stability on gust loads at transonic speeds. As an extension of this program, it was decided to increase the Mach number range of the tests to supersonic speeds.

A rough-air test was made on a tailless configuration having cruciform 60° triangular wings and covered the Mach number range of 0.84 to 1.67. This model was geometrically similar to the model of reference 3 which covered the Mach number range of 0.66 to 0.92. The model of the present test differed from that of reference 3 in weight, moment of inertia, and wing material.

CONFIDENTIAL

The test results for this model are evaluated in order to establish the characteristics of the loads and their variation with Mach number. In addition, comparisons are made of root-mean-square acceleration increments measured normal to each wing of the cruciform arrangement as in reference 3. Also, calculated values of the root-mean-square acceleration increment, obtained by the method and chart of reference 3, are compared with the experimental results.

SYMBOLS

a_n	normal-acceleration increment, g units
a_t	transverse-acceleration increment, g units
\bar{c}	mean aerodynamic chord, ft
I_Y	moment of inertia about transverse axis, slug-ft ²
I_Z	moment of inertia about vertical axis, slug-ft ²
K_a	constant in equation of turbulence spectrum
M	Mach number
S	wing area, sq ft
t	time, sec
U_{de}	derived gust velocity, ft/sec
W	weight, lb
ζ	damping ratio
σ	root-mean-square acceleration increment, g units
ω_n	undamped frequency of airplane short-period oscillation, radians/sec

MODEL AND INSTRUMENTATION

Model

The principal features of the model are shown in the drawing of figure 1 and the photograph of figure 2. The fuselage had a maximum diameter of 6.5 inches and was constructed of wood with a metal nose. The 60° triangular wings were 1/4-inch flat plate steel with beveled edges. The important characteristics of the model are listed in figure 1.

The dynamic stability characteristics of the model are presented in figure 3 in the form of damping ratio ζ and undamped short-period frequency ω_n . The results of figure 3 were obtained by using the stability data of reference 4 from $M = 0.80$ to 0.95 and the stability data of reference 5 from $M = 1.10$ to 1.70 along with the weight, inertia, and flight conditions for the model of the present test.

Instrumentation

The model instrumentation provided the following telemetered quantities: normal acceleration measured at the model center of gravity, transverse acceleration measured at the model center of gravity, and total pressure.

Ground instrumentation included a CW Doppler radar set for obtaining model velocity, a modified SCR-584 radar set for obtaining model position in space, and a rawinsonde for obtaining atmospheric conditions. In addition, spinsonde equipment was used for obtaining a measurement of model angular velocity in roll.

The airplane flown in preflight surveys was equipped with standard airspeed-acceleration recording instruments and also a one-channel telemeter which transmitted normal-acceleration measurements to the ground receiving station.

TEST PROCEDURE

Airplane Turbulence Survey

The atmospheric and turbulence conditions for forecasting and selecting a suitable test day are described in reference 1. The test day was chosen on the basis of weather forecasts for the Langley Pilotless Aircraft Research Station at Wallops Island, Va. As a final check on the suitability of turbulence conditions, an airplane survey was made

before the model test. Another airplane survey was made before and after the model test to provide a measurement of the variation of turbulence intensity with altitude.

Flight surveys along the firing course were made in increments of 500 feet from an altitude of 500 feet to 3,000 feet. The recorded airspeed-acceleration data at each altitude were evaluated to determine the gust velocities U_{de} in accordance with the revised gust-load formula of reference 6. Examination of the acceleration data at each altitude showed no consistent trend in variation with distance from the launching site; therefore, the entire run at each altitude was treated as one set of data in determining the variation of turbulence intensity with altitude. The gust velocity equaled or exceeded on the average in 1.0 and 0.1 mile of flight is shown in figure 4 as a function of altitude. Examination of figure 4 indicates that there was little variation in turbulence intensity with altitude. On the basis of the results of figure 4, the assumption is made in presenting the model test results that no corrections were necessary for variations in turbulence intensity with altitude.

Model Test

After the airplane survey, the model was ground launched at an elevation angle of 21° by means of a fin stabilized booster rocket motor. The model separated from the booster at booster burnout and experienced decelerating flight from a Mach number of 1.73 to 0.82. The model flight path was approximately parabolic with a maximum altitude of 3,100 feet.

Data-Reduction Procedure

Acceleration measurements at the model center of gravity were made normal to each wing of the cruciform configuration and are called normal and transverse acceleration. The telemeter record obtained from the model (samples of the record are shown in fig. 5) was read at 0.01-second time intervals resulting in a total of 2,500 data points for each accelerometer for the power-off portion of the flight over the Mach number range of 1.73 to 0.82. The time history of acceleration measurements was divided into sections as listed in table I. These record sections were analyzed to obtain power spectra and root-mean-square acceleration increments for each sample. In order to provide a variation of acceleration increment with Mach number the results of the data analysis are presented at an average Mach number for each record section. The Mach number and altitude change for each record section along with the average Mach number and altitude and the sample size are shown in table I.

RESULTS AND DISCUSSION

Characteristics of Model Rough-Air Response

Several samples of the telemeter record are shown in figure 5 for the transverse- and normal-acceleration measurements. In general, the time histories show that the model response is mainly at the short-period frequency with some indication of wing first bending frequency of 63 cps superimposed on the short-period oscillations.

Power-spectral-density functions of acceleration provide a better picture of the important frequencies present in the model rough-air response and are shown in figure 6 for several Mach numbers corresponding to the time histories of figure 5. Since the data were reduced from the telemeter records at 0.01-second intervals, the highest frequency that could be resolved was 50 cps. (See ref. 7.) Since the high-frequency components were not faired from the records before computing the spectra, the power densities at frequencies higher than 50 cps are reflected to a small amount in the lower frequencies. The spectra of figure 6 are roughly concentrated at the short-period frequency and the portion of the spectrum from 20 cps to 50 cps was negligible. The increase in short-period frequency with Mach numbers shown in figure 6 agrees very well with the variation of ω_n shown in figure 3.

Variation of Acceleration With Mach Number

The variation of root-mean-square acceleration increment with Mach number is presented in figures 7 and 8. The accelerations measured normal to each wing of the cruciform configuration (normal and transverse) are presented in figure 7. As stated in a previous section, no corrections have been made to the data for variations in turbulence intensity along the model flight path. Both σ_{an} and σ_{at} show a large increase between $M = 0.84$ and $M = 1.02$ and, within the scatter of the data, little variation between $M = 1.02$ and $M = 1.67$.

Under the assumption that the data of figure 7 are from two separate tests under the same turbulence conditions, σ_{an} and σ_{at} were combined

in figure 8 as follows: $\sigma = \sqrt{\frac{\sigma_{an}^2 + \sigma_{at}^2}{2}}$. The root-mean-square acceleration appears to increase from roughly 0.20g at a Mach number of 0.90 to 0.40g at a Mach number of 1.00, an increase of roughly 100 percent.

Of this 100-percent increase, roughly only 30 percent appears attributable to direct effects associated with speed increase and with the change in slope of the lift curve for this Mach number range. The remaining

70 percent appears to be essentially a reflection of the deterioration of damping over this Mach number range. These results are in good agreement with formula (8) of reference 3 which relates mean-square acceleration to the lift-curve slope, speed, and time to damp to one-half amplitude.

For comparison with the experimental results, calculated values of σ were obtained using the method and charts of reference 3 where the value of K_a necessary for making the calculations was determined from the airplane-survey data to be 0.033. The calculations appear to show the same trend with Mach number as the experimental data, with a sharp increase in σ between $M = 0.90$ and $M = 0.95$ associated with the decrease in damping in pitch illustrated in figure 3. Calculations were not made between $M = 0.95$ and 1.10 since dynamic stability data were not available at these Mach numbers from references 4 and 5. From $M = 1.10$ to $M = 1.70$, the calculated curve shows a small increase with Mach number which is within the accuracy or scatter of the experimental data. It should also be pointed out that the configurations of references 4 and 5 used to obtain the stability derivatives had wing airfoil sections of NACA 0004-65 and NACA 0003-63, respectively, while the model of the present test had flat plate wings with sharp leading edges.

The results from reference 3 for a similar rocket model tested in rough air are also shown in figure 8. The data from reference 3 have been corrected to the weight, inertia, and flight conditions of the present test. The data from the model of reference 3 show a somewhat similar trend with Mach number; however, the increase in σ occurs at a lower Mach number.

Comparison of a_n and a_t

Because of the short flights and the deceleration rate of the model, the sample sizes were limited as shown in table I. The effect of the short sample length at each test condition is to introduce statistical fluctuations in the data. The repeatability of the tests would give some indication of the accuracy of the results. As discussed in reference 3, some indication of the accuracy of the results is given by considering the results from each wing of the cruciform configuration to be a separate measurement of the gust-loads experience for the configuration. Comparisons are made of a_n and a_t in the time histories of figure 5, the power spectra of figure 6, and the root-mean-square accelerations of figure 7. The differences between the two values of σ shown in figure 7 are as small as ± 5 percent and as large as ± 16 percent of the average value of σ obtained from combining the two sets of data. From these results, it is felt that ± 20 percent is a reasonable figure for accuracy of the data presented.

CONCLUDING REMARKS

The present investigation has yielded information on the behavior of a tailless cruciform 60° triangular-wing configuration in rough-air flight from Mach numbers 0.84 to 1.67. The variation of root-mean-square acceleration increment with Mach number indicated a rapid increase of roughly 100 percent as the Mach number increased from 0.90 to 1.00. Of this 100 percent, about 70 percent appeared to be associated with the rapid decrease in pitch damping over this Mach number range. From Mach numbers of 1.02 to 1.67, the experimental data showed little variation with Mach number at least within the estimated accuracy of the results of ± 20 percent.

Langley Aeronautical Laboratory,
National Advisory Committee for Aeronautics,
Langley Field, Va., May 24, 1956.

REFERENCES

1. Vitale, A. James, Press, H., and Shufflebarger, C. C.: An Investigation of the Use of Rocket-Powered Models for Gust-Load Studies With an Application to a Tailless Swept-Wing Model at Transonic Speeds. NACA TN 3161, 1954.
2. Vitale, A. James: Characteristics of Loads in Rough Air at Transonic Speeds of Rocket-Powered Models of a Canard and a Conventional-Tail Configuration. NACA RM L54L17, 1955.
3. Vitale, A. James, and Mitchell, Jesse L.: Experimental Results From a Test in Rough Air at High Subsonic Speeds of a Tailless Rocket Model Having Cruciform Triangular Wings, and a Note on the Calculation of Mean Square Loads of Aircraft in Continuous Rough Air. NACA RM L55L28, 1956.
4. Beam, Benjamin H., Reed, Verlin D., and Lopez, Armando E.: Wind-Tunnel Measurements at Subsonic Speeds of the Static and Dynamic-Rotary Stability Derivatives of a Triangular-Wing Airplane Model Having a Triangular Vertical Tail. NACA RM A55A28, 1955.
5. Tobak, Murray: Damping in Pitch of Low-Aspect-Ratio Wings at Subsonic and Supersonic Speeds. NACA RM A52L04a, 1953.
6. Pratt, Kermit G.: A Revised Formula for the Calculation of Gust Loads. NACA TN 2964, 1953.
7. Tukey, John W.: The Sampling Theory of Power Spectrum Estimates. Symposium on Applications of Autocorrelation Analysis to Physical Problems (Woods Hole, Mass.), June 13-14, 1949, pp. 47-67. (Sponsored by ONR, Dept. Navy.)

TABLE I

VARIATION OF MACH NUMBER, SAMPLE SIZE, AND ALTITUDE

Mach number of sample	Sample size, number of points	Altitude, ft
1.672 ± 0.053	120	1,500 ± 200
1.563 ± .055	140	1,925 ± 225
1.450 ± .058	160	2,350 ± 200
1.335± .057	180	2,700 ± 150
1.225 ± .054	200	2,975 ± 125
1.117 ± .054	220	3,110 ± 10
1.016 ± .048	240	3,085 ± 35
.941 ± .027	260	2,900 ± 150
.896 ± .018	280	2,500 ± 250
.864 ± .014	300	1,900 ± 350
.838 ± .013	400	775 ± 775

CONFIDENTIAL

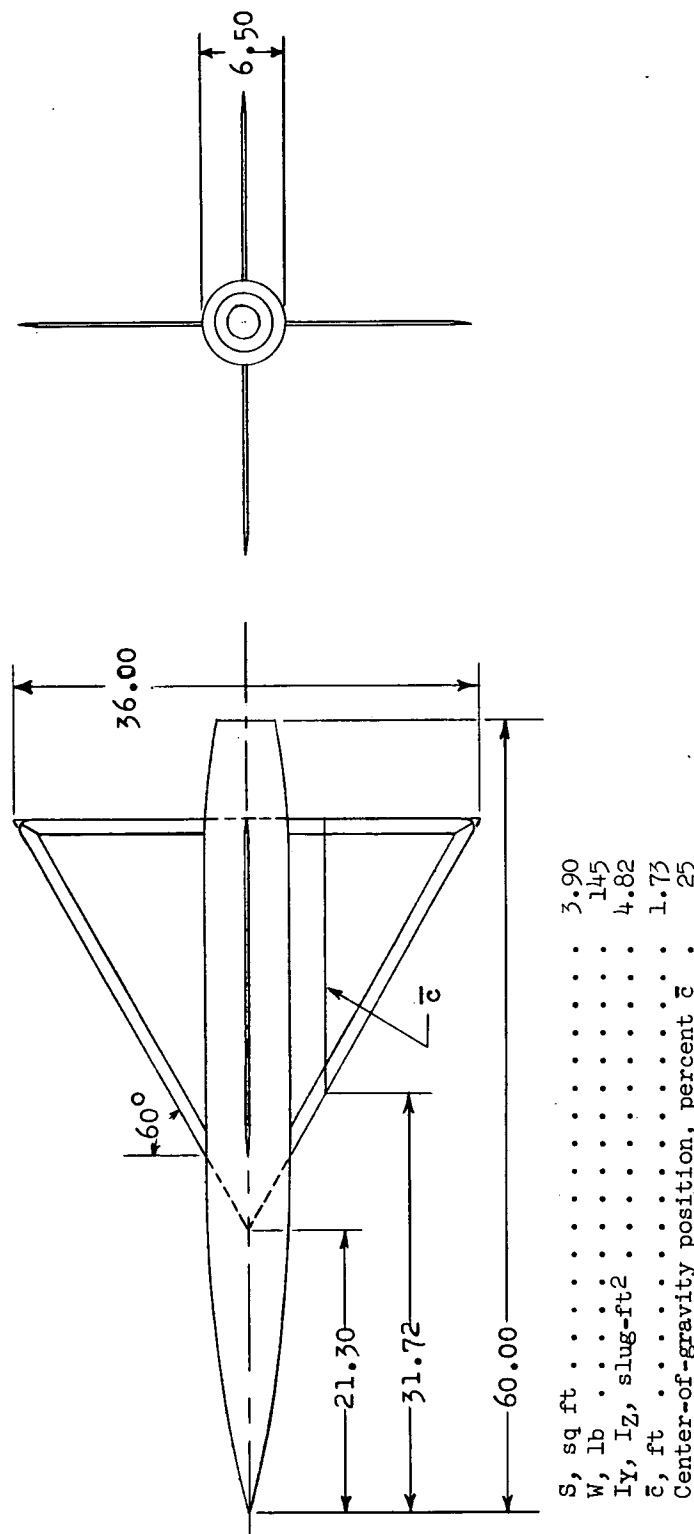


Figure 1.- Drawing of model. All dimensions are in inches.

L-87775•1

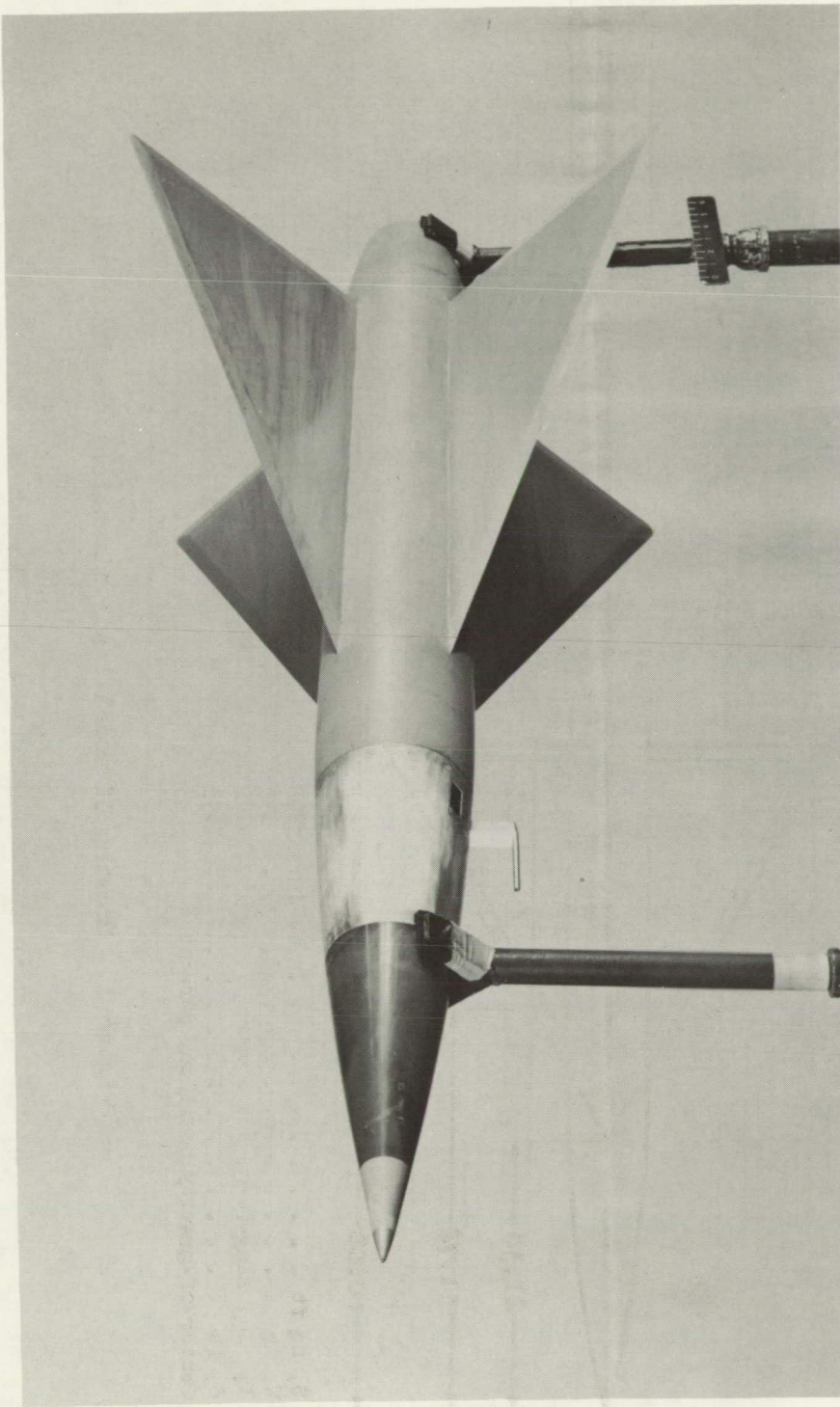
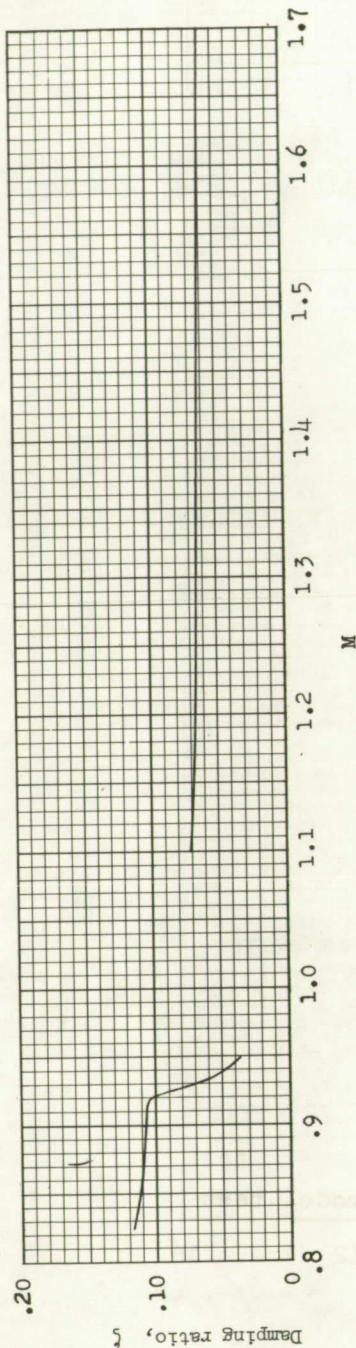
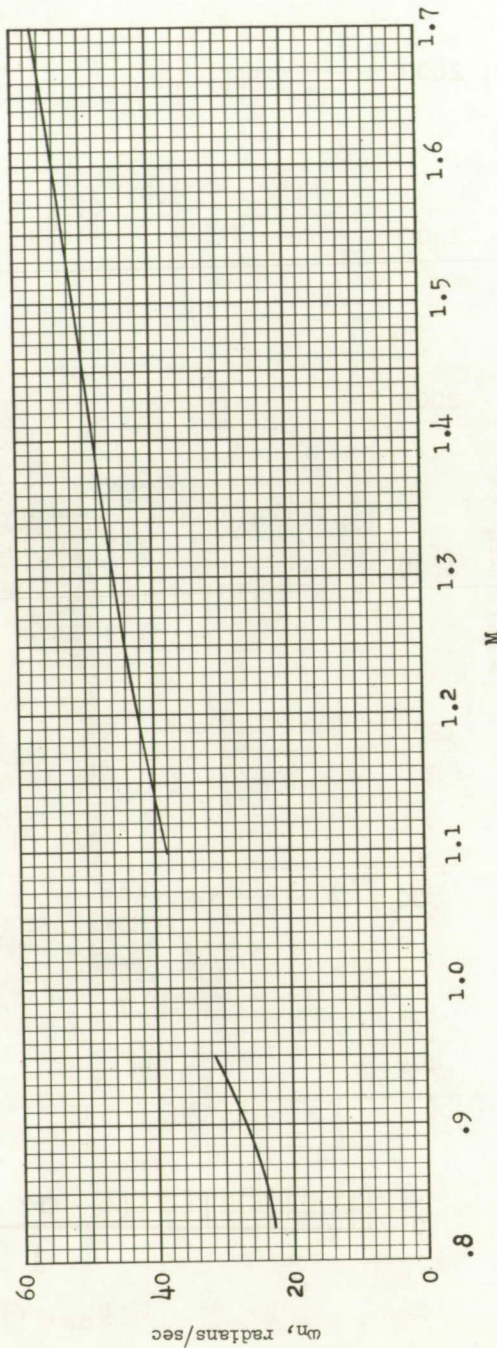


Figure 2.- Photograph of model.



(a) Variation of damping ratio with Mach number.



(b) Variation of undamped natural frequency with Mach number.

Figure 3.- Stability characteristics of model.

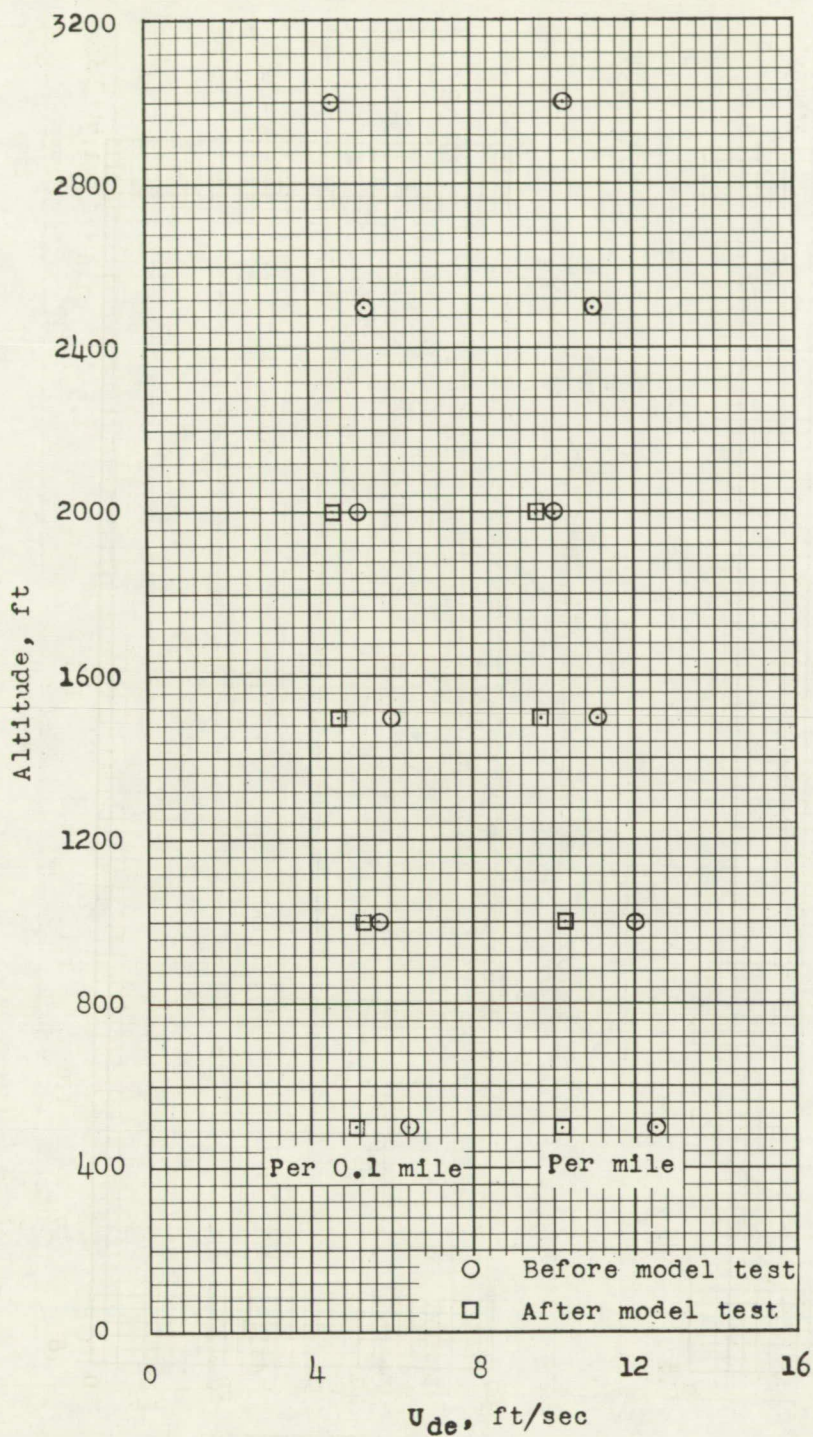


Figure 4.- Variation of gust intensity with altitude as indicated by the survey airplane.



Figure 5.- Time histories of acceleration.

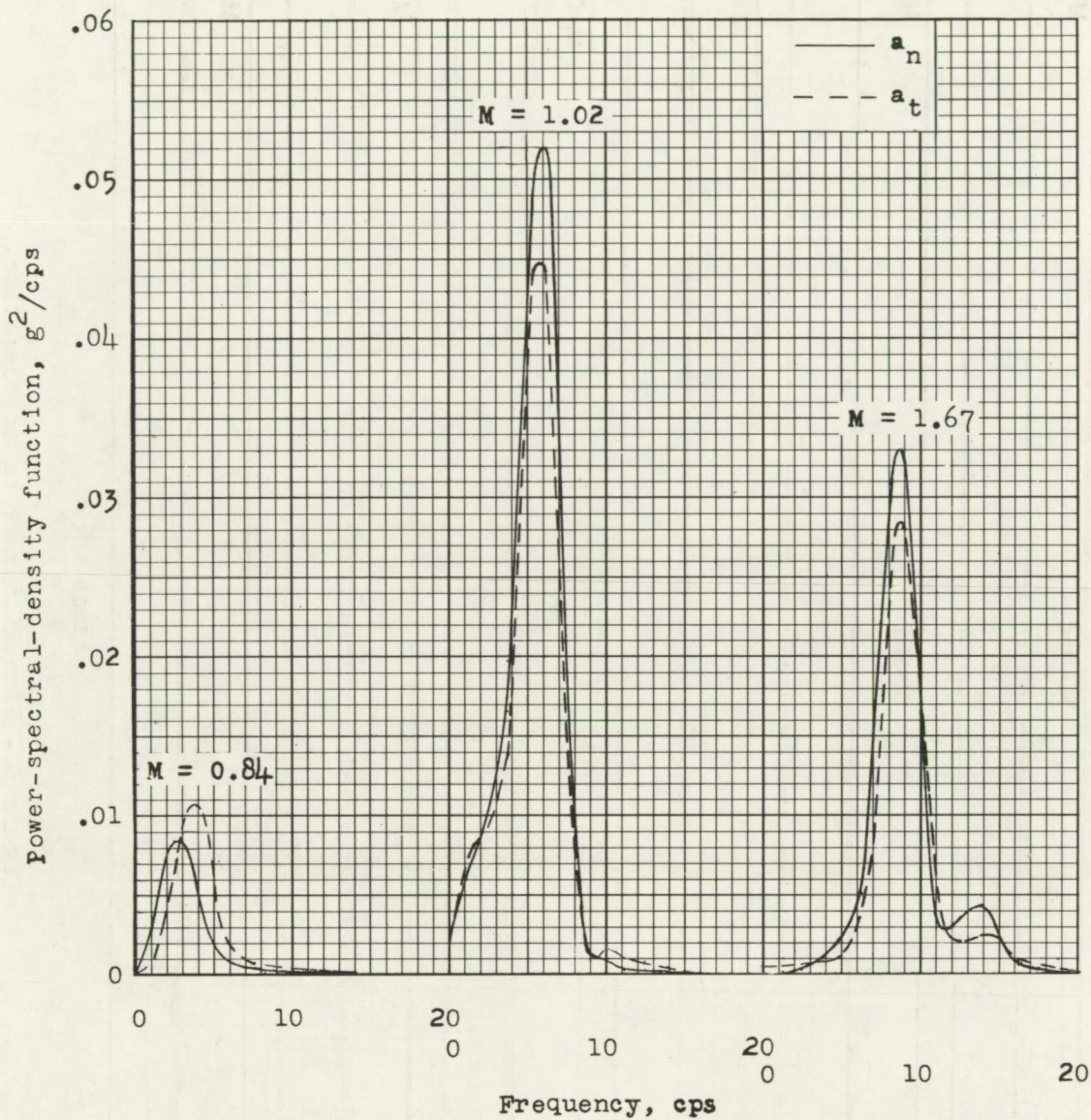


Figure 6.- Power-spectral-density functions of acceleration.

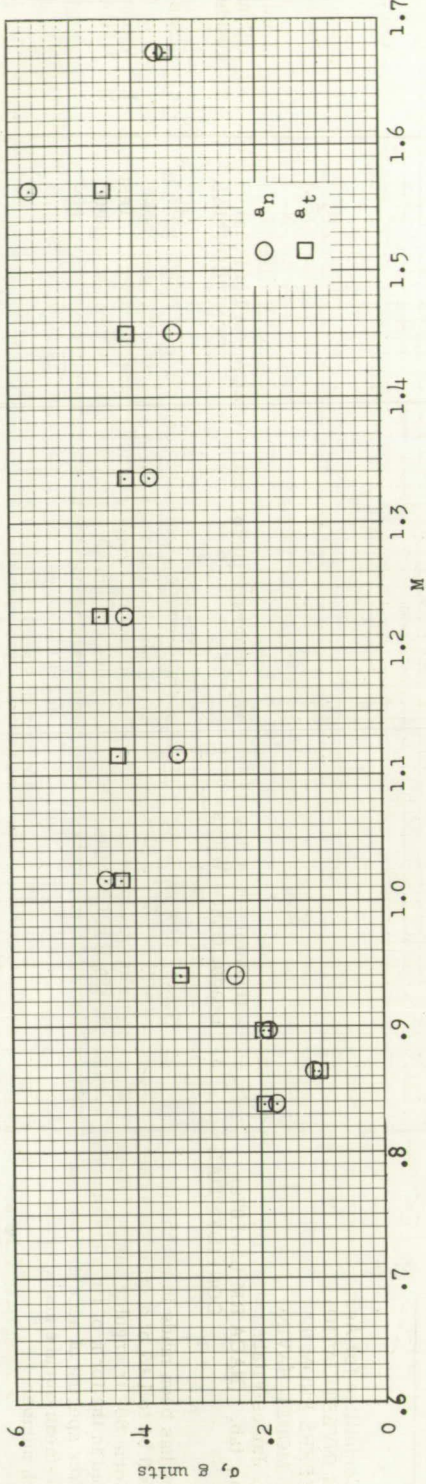


Figure 7.- Comparison of normal and transverse root-mean-square acceleration.

